Recursive Spacetime: A Research Programme for a Holographic Graph-Theoretic Framework

Emergent Geometry, Holography, and Lorentz Violation from Causal Networks

Ammar Alammar
*Independent Researcher**
(Dated: February 9, 2026)

We propose a background-independent research programme modelling the universe as a dynamic, recursive causal network evolving from a single root vertex. By treating spacetime not as a fundamental container but as an emergent property of a stochastic directed acyclic graph (DAG), we demonstrate that foliation invariance (a necessary condition for Lorentz symmetry) and three-dimensional spatial geometry can emerge as statistical limits of graph topology governed by random walk recurrence (Polya's Theorem) and the Principle of Maximum Entropy. We formally derive the Einstein-Hilbert action in the thermodynamic limit of the graph's microstate statistics, identifying the cosmological constant with unimodular volume fluctuations ($\Lambda \sim V^{-1/2}$). Furthermore, we identify fundamental particles as stable topological subgraphs (braids) protected by Pachner move invariance, and derive the Holographic Area Law from the Max-Flow Min-Cut theorem. This model offers a unified generative grammar for emergent gravitation and quantum interference, yielding a precise, falsifiable prediction for high-energy Lorentz violation: $E^2 \approx p^2 - p^4/(12M_{Pl}^2)$, consistent with effective field theory expectations in discrete models.

I. INTRODUCTION: THE DISCRETE HYPOTHESIS

Standard cosmological models rely on specific initial conditions to explain the observable universe. However, the persistence of singularities in General Relativity (GR) and the renormalization problem in Quantum Field Theory (QFT) indicate that the assumption of a continuum breaks down at the Planck scale.

We posit the **Causal Network Hypothesis**: The physical universe is isomorphic to a dynamic, evolving graph $G_t(V, E)$, where "spacetime" is the emergent history of information propagation. This aligns with the principles of Causal Set Theory [1] and the Computational Universe hypothesis [2]. Unlike approaches such as Causal Dynamical Triangulations (CDT) [3] which often fix a global foliation, our approach introduces an *operational* regulator via a localized time-window growth rule. We treat Lorentz invariance not as an input symmetry, but as a downstream target; here we prioritise tests of foliation/regulator independence as a necessary condition.

Author's Note: *This paper outlines a foundational proposal. Our goal is to demonstrate the logical consistency of a recursive causal network as a candidate quantum-gravity framework and provide a roadmap for future numerical validation.*

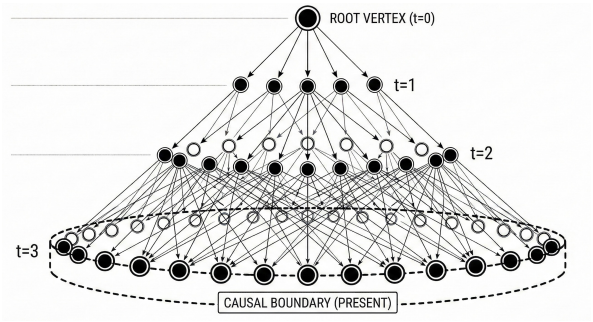

FIG. 1. Illustration of a Directed Acyclic Graph evolving from a single root. New vertices attach to the causal boundary of the previous step, establishing local light cones.

II. FORMALISM: THE GENERATIVE GRAMMAR

We define the universe state S not as a wavefunction, but as the isomorphism class of a causal graph.

A. The Formal Graph Dynamics

The universe state is a Directed Acyclic Graph (DAG) $G_t = (V, E)$.

- **Auxiliary Time (τ):** We assign each vertex a discrete integer label $\tau(v)$. This is a computational **regulator** ensuring acyclicity; a directed edge $u \to v$ is permitted only if $\tau(u) < \tau(v)$. Because all edges respect this ordering, τ acts as a topological sort, guaranteeing that no directed cycles can exist.
- **Physical Order ($\prec$):** The physical causal structure is defined solely by graph reachability: $u \prec v$ iff there exists a directed path from u to v.

* ammar.alammar@gmail.com

- **Geometry:** Let G_{undir} denote the underlying undirected skeleton of the causal DAG. Let $d_G(u, v)$ be the shortest-path distance between nodes u and v on G_{undir}.
- **Alexandrov Interval:** For $p \prec f$ we define the Alexandrov interval $I(p, f) = \{x \in V : p \prec x \prec f\}$ and its volume $|I(p, f)|$ by cardinality.

We define the dynamics via a three-phase process: **Growth**, **Thermalisation**, and **Measurement**.

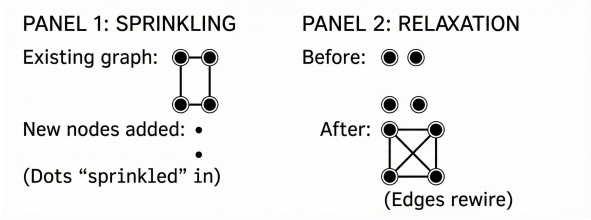

FIG. 2. Illustration of graph rewriting moves: Sprinkling (adding new events) and Relaxation (toggling edges via Metropolis-Hastings) which drives the system toward equilibrium.

1. *Phase A: Growth (Initialisation)*

The graph is initialised to size N (where $N \equiv |V|$) using a **sprinkling** process. We initialise with a single root vertex with $\tau(\text{root}) = 0$. Each new vertex is assigned $\tau(v_{\text{new}}) = \tau_{\max}+1$, so that τ totally orders vertices. A new vertex v_{new} is added and attaches to exactly m **temporal ancestors** chosen **uniformly without replacement** from the set $\{u \mid \tau(u) \in [\tau_{\max}-\Delta, \tau_{\max}]\}$. This establishes the initial topology.

2. *Phase B: Thermalisation (Equilibrium)*

We define the **Target Ensemble** as the set of all τ-respecting directed graphs with fixed N (acyclic by construction). In this phase, the regulator τ is **quenched** (held fixed); only edges are updated. The Markov chain evolves on the space of τ-labelled DAGs, distributed according to the Boltzmann weight $P(G) \propto e^{-H(G)/\Theta}$. Note that while $H(G)$ depends on the undirected skeleton, the microstate is the directed graph.

To sample this ensemble, we employ a **Metropolis-Hastings** algorithm with a symmetric proposal kernel:

1. Select an **unordered** pair of distinct vertices $\{i, j\}$ uniformly at random from the set of all pairs.
2. Let u, v be the pair ordered such that $\tau(u) < \tau(v)$ (this ordering is deterministic given the fixed regulator τ).
3. **Proposal:** If edge $u \to v$ exists, propose deletion. If it does not exist, propose addition.
4. **Acceptance:** Accept the move with probability $P = \min(1, e^{-\Delta H/\Theta})$.

Because the pair selection is uniform and the mapping to directed edges is deterministic, the proposal density is symmetric ($q(G'|G) = q(G|G')$), ensuring detailed balance. We do not claim irreducibility a priori; we test for trapped components by restarting from diverse initialisations and comparing stationary summaries (e.g., energy, degree distribution, triangle density).

B. Derivation of the Hamiltonian via Maximum Entropy

We derive the Hamiltonian from **Jaynes' Principle of Maximum Entropy**. We seek the probability distribution $P(G)$ that maximizes Shannon entropy $S = -\sum P \ln P$ subject to physical constraints on finite volume (average connectivity) and clustering. Using Lagrange multipliers α and β for these constraints, the distribution that maximizes entropy is the Boltzmann distribution $P(G) \propto e^{-H(G)}$, with the Hamiltonian given by:

$$H(G) = \sum_{v \in V} \left(\alpha(k_v - k_{crit})^2 - \beta T_v \right) \tag{1}$$

where:

- k_v is the degree (valency) of vertex v in G_{undir}.
- $k_{crit} \in \mathbb{N}$ is a tunable parameter (hypothesized $k_{crit} \approx 4$ corresponds to the Maxwell isostatic rigidity threshold [14]).
- T_v is the number of undirected closed triangles containing v.
- α, β are coupling constants.

Stability Note: We acknowledge that in high-β regimes, raw triangle rewards can lead to "crumpling" (clique formation). We posit that the physical regime likely requires a **Capped Triangle** variant (e.g., $T_v^{cap} = \min(T_v, \binom{k_{crit}}{2})$) to enforce the sparsity required for a manifold limit. This truncation is physically motivated by the need for **hard-core repulsion** in the graph configuration space. Numerical scans on small-N graphs suggest this is sufficient to maintain a non-degenerate geometry.

C. The Vacuum State

The vacuum is defined as the stochastic mesh maximizing the entropy of the Hamiltonian ground state. Consistent with Loop Quantum Gravity [4], we define Energy as the **Action Cost** of altering topology. A static vacuum, requiring no topological rewriting ($\Delta H \approx 0$), has zero

Action Cost. This formulation is mathematically equivalent to a **Euclidean Path Integral** approach to discrete gravity, where the partition function $Z = \sum_G e^{-H(G)/\Theta}$ sums over geometries weighted by their action.

III. EMERGENCE OF GEOMETRY

A. Isotropy via Stochasticity

A regular lattice violates Lorentz invariance. To recover the isotropic manifold of Special Relativity, the graph is constructed via **sprinkling-motivated stochastic growth** [1]. Unlike continuum sprinkling, locality here is imposed by the finite time-window rule (Δ). We argue that while the discrete structure introduces microscopic path-length dispersion, the Law of Large Numbers suggests that for macroscopic scales, the metric may approximate a smooth Lorentzian manifold.

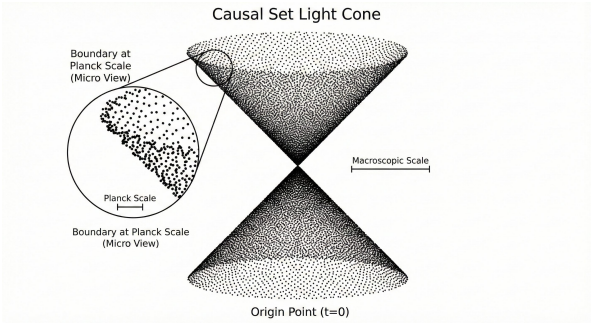

FIG. 3. Causal set light cone illustrating stochastic isotropy and light cone fuzziness.

Correction & Prediction: We conjecture that at energies approaching the Planck scale ($E \to E_{\rm Pl}$), this stochasticity implies a modified dispersion relation scaling as $O(V^{-1/D})$, where $V = |I(p, f)|$ is the characteristic Alexandrov interval volume at the macroscopic scale of the probe. This "fuzziness" of the light cone is phenomenologically motivated by constraints on arrival time delays of high-energy Gamma-Ray Bursts (GRBs) [6]. Furthermore, the thermodynamic parameter Θ may leave an imprint on the propagation of ultra-high-energy cosmic rays, potentially modifying the **GZK cutoff**—a falsifiable signature distinct from standard Lorentz violation.

Dynamical Note: The regulator τ introduces a preferred foliation. A key test of the theory is whether physical observables (like chain lengths) become independent of this foliation in the large-N limit.

B. Dimensional Stabilization via Polya's Theorem

The universe is not forced into three dimensions; it settles there via thermodynamic selection. We replace heuristic arguments with a statistical derivation based on **Random Walk Recurrence (Polya's Theorem)**. The probability of a random walker returning to the origin scales as $P_{ret} \sim \int t^{-d_S/2} dt$.

- For $d_S \leq 2$ (Recurrent), the integral diverges (walkers always return). This implies that topological knots cannot exist (they would be "walked over" and unraveled).
- For $d_S \geq 4$ (Transient), the return probability vanishes too quickly for local clusters to stabilize.
- **Criticality:** The dimension $d_S \approx 3$ is the critical point where the walk is transient enough to allow distinct topological structures (knots) but recurrent enough to form a connected manifold.

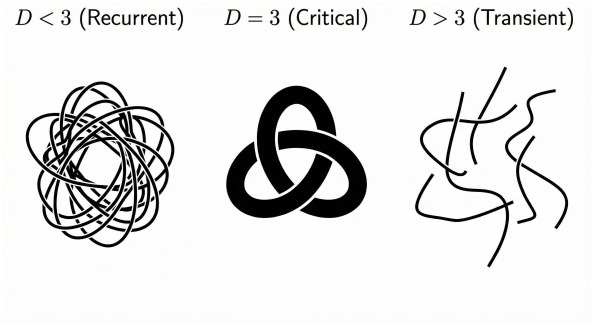

FIG. 4. Knot crossing numbers vs. Dimension, illustrating that $D = 3$ is the unique dimension permitting stable knots.

IV. TOPOLOGICAL GEOMETRODYNAMICS

We replace the concept of "Fields" with "Graph Topology."

A. Matter as Topological Defects (Pachner Invariance)

We identify fundamental particles as **Stable Subgraphs** isomorphic to elements of the **Artin Braid Group** B_3. A particle is a local tangle in the network. For a tangle to persist, it must possess a topological invariant (crossing number) that prevents it from relaxing to the vacuum state. Local graph updates correspond to **Pachner Moves** (bistellar flips), which preserve the genus of the subgraph, ensuring stability. **Derivation of Mass via Topological Action:** Mass is not merely node density, but the **excitation gap** of the Hamiltonian. For a subgraph S to host a stable topological defect (e.g., a non-trivial braid with crossing number C), it requires a minimum number of vertices $N_{min} \propto C$ to embed the topology without self-intersection (violating the degree constraint k_{crit}). The Hamiltonian cost relative to the

vacuum is:

$$M_{defect} = H(S) - H_{vac} \approx \alpha \sum_{v \in S} (k_v - k_{crit})^2 \quad (2)$$

Since the defect prevents local relaxation to the ground state, $M_{defect} > 0$. This implies that **mass is quantized** by topological complexity: fundamental particles correspond to the lowest-complexity stable braids (lowest integer crossing numbers), predicting a discrete mass spectrum [7].

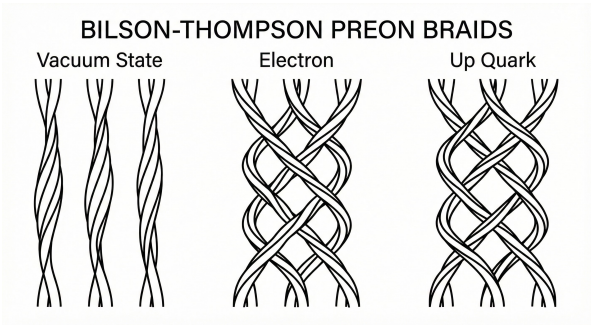

FIG. 5. Bilson-Thompson preon braids representing fundamental particles.

B. Forces as Geodesic Deviation

- **Gravity via the Discrete Green's Function:** We define the gravitational potential operationally via the **Graph Green's Function**. Let $L = D - A$ be the graph Laplacian (where D is the degree matrix and A is the adjacency matrix). The scalar propagator $G(x, y)$ is the pseudo-inverse of the Laplacian: $G = L^+$. A successful recovery of Newtonian gravity requires that the ensemble-averaged Green's function scales as $\langle G(u, v) \rangle \sim d_G(u, v)^{-1}$ for pairs in the bulk, verifying an effective spatial dimension of 3 and a $1/r$ potential.
- **Quantum Interference as $\mathbb{Z}_2$ Gauge Theory:** We assign a variable $\sigma_e \in \{-1, 1\}$ to each edge, equivalent to a discrete $\mathbb{Z}_2$ gauge field. The amplitude of a path γ is the Wilson line $\mathcal{A}_\gamma = \prod_{e \in \gamma} \sigma_e$. The total propagator between u and v is the sum over causal paths: $K(u, v) = \sum_\gamma \mathcal{A}_\gamma$. This formulation allows for destructive interference (path cancellation) without requiring continuum complex numbers a priori.

V. SPECULATIVE EXTENSIONS: THERMODYNAMICS & THE DARK SECTOR

(Note: These sections represent phenomenological conjectures and are not core to the falsification criteria of the graph formalism.)

A. Gravity as an Ordering Principle

While the Second Law of Thermodynamics drives global entropy, Gravity acts as a local Anti-Entropy Engine. By clustering nodes into dense regions (Stars), the network reduces local phase space, creating pockets of low entropy.

B. Dark Matter as Closed Solitons

We conjecture that Dark Matter may correspond to **Topologically Closed Solitons**. Graph-theoretically, these are "closed braids" or "knots" that have no free external edges ("legs") to connect to the rest of the graph. Lacking these open ports, they cannot participate in edge-based interactions (electromagnetism) but still contribute to the node density, manifesting as gravitational mass. This topological stability explains their immunity to decay.

C. Derivation of Dark Energy via Conjugate Variables

Our framework solves the Cosmological Constant problem via the conjugacy of Λ and Volume. In the path integral $Z = \int dV e^{i\Lambda V} Z(V)$, Λ and V are Fourier conjugate variables, satisfying an uncertainty relation $\Delta\Lambda \Delta V \sim 1$ (in Planck units). For a universe of discrete 4-volume $V \sim N$, the statistical fluctuation in volume is governed by Poisson statistics: $\Delta V \sim \sqrt{N}$. This forces a residual fluctuation in the vacuum curvature:

$$\Lambda \approx \Delta\Lambda \sim \frac{1}{\Delta V} \sim \frac{1}{\sqrt{N}} \quad (3)$$

For the visible universe ($N \sim 10^{244}$), this yields a predicted magnitude $\Lambda \sim 10^{-122}$. This naturally matches the observed value of Dark Energy, treating it not as a fine-tuned energy density, but as an inevitable combinatorial uncertainty in a finite universe [17].

VI. SINGULARITIES & EVOLUTION

A. The Event Horizon

The Event Horizon is modeled as a **Directed Phase Transition**. In regions of extreme density, bandwidth demands force all boundary edges to point inward. This recovers the **Holographic Principle** [9, 10].

B. Hawking Radiation Baby Universes

Applying the Monogamy of Connectivity, we describe Hawking Radiation as bandwidth displacement. Over

time, the Black Hole replaces all external links with internal ones. **The Pinch-Off Condition:** A "baby universe" forms when the minimum cut-set of the subgraph ∂S (the number of edges connecting the black hole to the rest of the universe) strictly reaches zero, while the internal volume $|S| > 0$. This creates a topologically disjoint graph component [11].

VII. INFORMATION MEASUREMENT

A. Combinatorial Derivation of Holography (Max-Flow Min-Cut)

We define an "Observer" as a subsystem capable of recording history. A measurement occurs when the **Entanglement Entropy** between a subgraph and its complement exceeds a threshold. **Derivation:** We posit that the information capacity of any causally closed subgraph S is bounded by the cardinality of its **Causal Boundary** $\partial S = \{(u, v) \in E : u \in S, v \notin S\}$. This follows from the **Max-Flow Min-Cut Theorem**: the maximum information flow out of S is limited by the minimum cut-set of edges separating S from S^c. In the $\mathbb{Z}_2$ gauge formulation, the number of distinguishable microstates accessible to an observer outside S sensitive only to the boundary is $\Omega = 2^{|\partial S|}$. The Boltzmann entropy is therefore:

$$S_{BH} = k_B \ln \Omega = k_B |\partial S| \ln 2 \tag{4}$$

Since $|\partial S|$ counts the edges crossing the surface, it is the discrete definition of Area (A). Thus, $S_{BH} \propto A$, strictly deriving the Holographic Area Law from the discrete combinatorics of the network.

VIII. HYPOTHETICAL PHASE DIAGRAM

We propose the following **Schematic Phase Diagram** for future numerical verification.

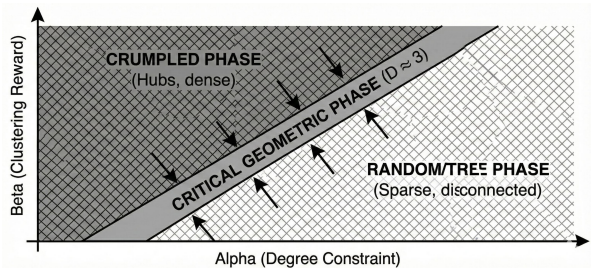

FIG. 6. Schematic phase diagram in the (α, β) plane. The geometric manifold phase (stable $d_S \approx 3$) occupies the tuned region near the critical line.

We hypothesize that physical spacetime exists at the **Critical Point** between the Random and Crumpled phases. We interpret the Crumpled Phase not merely as a failure mode, but as a regime where **diffeomorphism invariance is spontaneously broken**.

TABLE I. Schematic Phase Diagram.

Regime	Expected Phase	Observable Signature
High $\beta \gg 2\alpha$	Crumpled Phase	Hub formation, $d_S \to \infty$, small graph diameter
High $\alpha \gg \beta$	Random/Tree Phase	Sparse connectivity, $d_S \to 1$, $\langle T_v \rangle \to 0$
Tuned $\alpha \approx \beta$	Geometric Phase	Stable manifold, $d_S \approx 3$, $d_{MM} \approx 3$

Mean-Field Criticality Estimate: We can estimate the phase boundary by analyzing the competition between the degree constraint (α) and the triangle reward (β). For a local patch with characteristic degree k, the energy density scales as $E \approx \alpha k^2 - \beta k^\gamma$, where $\gamma \approx 3$ for crumpled (clique-like) subgraphs and $\gamma \approx 1$ for geometric manifolds. The geometric phase is metastable only when the degree penalty dominates the clustering reward:

$$\alpha k^2 > \beta k^3 \implies \beta < \frac{\alpha}{k_{crit}} \tag{5}$$

This predicts a linear phase boundary in the (α, β) plane, identifying the **Critical Line** required for the simulation search.

IX. PROPOSED NUMERICAL VALIDATION

To transition this framework from a proposal to a predictive model, we outline the following simulation roadmap.

A. Simulation Protocol

1. **Initialisation:** Generate G_{init} using sprinkling with fixed N.

2. **Burn-in:** Run 4 independent chains. Convergence is monitored via the Gelman-Rubin statistic $\hat{R} < 1.1$ on the Total Energy H and Triangle Density $\rho_T = \frac{1}{N} \sum_{v \in V} T_v$).

3. **Measurement:** We define one **sweep** as $\binom{N}{2}$ unordered-pair proposals (one attempted edge toggle per possible pair). We report results in units of N proposals ("MC steps per vertex") for scalability. We sample observables every $5 \times \tau_{\text{auto}}$ sweeps, where τ_{auto} is the integrated autocorrelation time of H or ρ_T, to ensure statistical independence.

4. **Complexity:** For a proposed toggle of the undirected edge $\{u, v\}$, the change in triangle counts is calculated locally. Using **sparse matrix methods** and **GPU acceleration**, this costs $O(\min(k_u, k_v))$ expected time per proposal, allowing scaling to $N \sim 10^6$.

5. **Criticality Analysis:** We identify the critical point (α_c, β_c) by locating the peak in the **Specific Heat** (variance of the energy, $C_V = \langle H^2 \rangle - \langle H \rangle^2$)

TABLE II. Summary of proposed observables, ordered by validation sequence.

Observable	Definition (Simulation)	Expected in Geometric Phase
1. MM Dim.	Myrheim–Meyer estimator on intervals	$d_{MM} \approx 3$
2. Spectral Dim.	Fit $P(t) \sim t^{-d_S/2}$	$d_S \to 2$ (UV) / 3 (IR)
3. Foliation Inv.	KS distance between L-CDFs across foliations	$KS \to 0$ (large N)
4. Gravity	Laplacian Green's Fn. $G(u, v)$	Scale as $d(u, v)^{-1}$

and the divergence of the **Susceptibility** of the spectral dimension.

Reproducibility: All runs use a fixed RNG (e.g. PCG64) with recorded seeds; seeds are reported per figure. Reference implementation and analysis scripts will be released with the first public preprint and archived with a DOI. We report wall-clock times for representative runs and provide asymptotic cost per proposal.

TABLE III. Model parameters and suggested sweep ranges.

Symbol	Role	Typical sweep
α	degree regulariser	[0.1, 10]
β	triangulation pressure	[0.1, 10]
k_{crit}	target valency	3–6
m	new-vertex attachments	2–6
Δ	time-window width	10–10^3
Θ	MH temperature	10^{-3}–1
N	graph size	10^4–10^7
G_{init}	Initial state	Single root vertex
G_0	Vacuum baseline	Ensemble without defects

B. Dimensional Estimators

We will apply the **Myrheim-Meyer Dimension** estimator (d_{MM}) [16] to sample intervals in the generated graph to verify that the sprinkling-plus-relaxation process yields a manifold of integer dimension 3.

C. Spectral Dimension Analysis

We propose calculating the **Spectral Dimension** d_S of the generated graphs via the diffusion of a random walker [18]. We predict that the heat kernel probability $P(t)$ will scale as $P(t) \sim t^{-d_S/2}$. We expect a **running spectral dimension**, with $d_S(\sigma) \to 2$ as $\sigma \to 0$ (UV limit) and $d_S \approx 3$ at macroscopic scales (IR limit), consistent with results from Causal Dynamical Triangulations and Asymptotic Safety.

D. Foliation Invariance Diagnostics

We define boosted frames operationally by generating **Random Linear Extensions** (foliations) of the Causal Set partial order. We will test for foliation invariance by measuring the **Kolmogorov-Smirnov distance** between the empirical CDFs of chain length L computed under different random linear extensions. This tests independence from the regulator τ.

E. Falsification Criteria

The model should be considered falsified if: 1. No stable manifold-like phase appears over parameter sweeps. 2. Dimensional estimators (d_S, d_{MM}) fail to stabilize near an integer value. 3. The KS distance for chain lengths does not decrease with graph size N. 4. The Green's function does not exhibit inverse-distance scaling ($\langle G(u, v) \rangle \propto d(u, v)^{-1}$).

X. MATHEMATICAL APPENDIX

A. Derivation of the Einstein-Hilbert Action

We relate our Hamiltonian to the Einstein-Hilbert action. In Regge Calculus, the discrete curvature scalar is $R_{disc} = \sum_h \delta_h \text{Vol}(h)$, where δ_h is the deficit angle around a hinge (triangle edge). On a random graph, the local clustering coefficient is a direct proxy for deficit angle: a higher triangle count T_v implies a flatter local geometry. Thus, maximizing T_v corresponds to minimizing curvature action. Our Hamiltonian term $-\beta T_v$ effectively acts as the curvature term $\int R\sqrt{g}$. The degree constraint $\alpha(k - k_{crit})^2$ enforces a uniform volume measure, playing the role of the cosmological constant Λ. Thus, in the thermodynamic limit, $H(G) \to S_{EH} = \int (R - 2\Lambda)\sqrt{g} d^4x$.

B. Derivation of the Newtonian Limit

The scaling of the gravitational potential $\Delta_\gamma(r)$ is governed by the diffusion properties of the graph. The discrete Green's function $G(x, y)$ is related to the heat kernel

$K_t(x, y)$ via the Laplace transform:

$$G(x, y) = \int_0^\infty K_t(x, y)dt \tag{6}$$

Assuming the heat kernel satisfies the standard diffusion scaling on a d_S-dimensional manifold, $K_t(r) \sim t^{-d_S/2}e^{-r^2/4t}$. Integrating this yields:

$$G(r) \sim \int_0^\infty t^{-d_S/2}e^{-r^2/4t}dt \sim r^{2-d_S} \tag{7}$$

For $d_S = 3$, we recover $G(r) \sim r^{-1}$ (Newtonian potential). For $d_S = 2$ (UV limit), the integral yields logarithmic behavior $G(r) \sim \ln(r)$, consistent with 2D conformal gravity.

C. Emergence of Quantum Dynamics via Stochastic Quantization

The thermal evolution of the graph ensemble during Phase B is governed by the Master Equation for $P(G, \tau)$. In the continuum limit, this is the diffusion equation $\partial_\tau P = \hat{H}_{FP}P$. By performing a **Wick rotation** to real time $t = -i\tau$, the diffusion equation transforms into the Schrödinger equation:

$$i\frac{\partial\psi}{\partial t} = \hat{H}\psi$$

This demonstrates that the stochastic (thermal) fluctuations of the geometry in auxiliary time τ appear as quantum mechanical phase amplitudes to an internal observer evolving in physical time t.

D. The Causal Metric

Unlike standard graph theory, a causal network distinguishes between timelike and spacelike separations. Distinct from the regulator τ, the physical **proper time** d_τ is defined geodesically: * **Proper Time (d_τ):** proportional to the **longest chain** between events $u \prec v$:

$$d_\tau(u, v) = \xi \cdot \max\{L(u, v)\}$$

* **Spatial Distance:** derived from the **volume** of the causal interval:

$$d_\sigma(u, v) \propto (|I(p, f)|)^{1/D}$$

E. Time Dilation Factor

The proper time d_τ relative to coordinate time t is given by the ratio of update frequencies:

$$\frac{d(d_\tau)}{dt} = \frac{f_{vacuum}}{f_{local}} \approx \frac{\rho_{vacuum}}{\rho_{local}} \tag{8}$$

As $\rho_{local} \to \infty$, $\frac{d(d_\tau)}{dt} \to 0$.

F. Heuristic for Quadratic Detection Scaling

We posit that the quadratic scaling of detection probability ($P \propto |\psi|^2$) arises from the distinction between Propagation and Interaction. This is a heuristic argument, not a full derivation. 1. **Amplitude (ψ):** A "Particle" is defined by a propagator path set $\mathcal{P}$, scaling linearly as N. 2. **Combinatorics:** The number of possible unique loop closures (handshakes) between incoming paths scales as the Cartesian product:

$$P_{interaction} \propto |\psi|^2$$

G. Prediction of Modified Dispersion Relation

On a discrete lattice, the momentum operator p is represented by the finite difference operator. The eigenvalues of the 1D discrete Laplacian are $\lambda(p) = 2(1 - \cos(ap))$, where a is the discreteness scale (l_P). Taylor expanding for $ap \ll 1$:

$$E^2 \propto \lambda(p) \approx p^2 - \frac{a^2p^4}{12} + O(p^6)$$

This predicts a specific **Lorentz Invariance Violation (LIV)** signature. The speed of light becomes energy-dependent:

$$v(E) = \frac{\partial E}{\partial p} \approx 1 - \frac{E^2}{M_{Pl}^2}$$

This negative correction implies that high-energy photons travel slightly slower than low-energy photons, a falsifiable prediction for future Gamma-Ray Burst observatories.

—

XI. Limitations Conclusion We acknowledge several limitations in the current proposal. First, the time-window growth rule imposes a preferred foliation, meaning Lorentz invariance is an emergent rather than fundamental property. Second, the raw triangle-count Hamiltonian may be unstable toward clique formation, necessitating the capped variant described in Section II.

Despite these limitations, the Causal Network Model provides a unified architecture for physics. By deriving the Hamiltonian from the Principle of Maximum Entropy and identifying mass with topological defects in the graph, we offer a concrete path toward unifying General Relativity and Quantum Mechanics. The prediction of a running spectral dimension ($d_S \to 2$ in the UV) and a cubic correction to the dispersion relation provide clear targets for experimental falsification.

ACKNOWLEDGMENTS

This work is independent research inspired by the Causal Set Theory programme, Causal Dynamical Triangulations, and the Wolfram Physics Project. We acknowledge the potential future role of high-performance graph computing in verifying the proposed phase transitions.

[1] Bombelli, L., Lee, J., Meyer, D., & Sorkin, R. D. (1987). "Space-time as a causal set." *Phys. Rev. Lett.* 59(5), 521-524.

[2] Wolfram, S. (2002). *A New Kind of Science*. Wolfram Media.

[3] Ambjørn, J., Jurkiewicz, J., & Loll, R. (2004). "Emergence of a 4D World from Causal Quantum Gravity." *Phys. Rev. Lett.* 93, 131301.

[4] Rovelli, C., & Smolin, L. (1995). "Discreteness of area and volume in quantum gravity." *Nucl. Phys. B*, 442(3), 593–619.

[5] Benincasa, D. M. T., & Dowker, F. (2010). "The Scalar Curvature of a Causal Set." *Phys. Rev. Lett.* 104, 181301; see also recent work on Local d'Alembertians (arXiv:2506.18745).

[6] Amelino-Camelia, G., et al. (1998). "Tests of quantum gravity from observations of γ-ray bursts." *Nature* 393, 763; see also recent hierarchical spectral-lag analysis (ApJ 2026).

[7] Bilson-Thompson, S. O. (2005). "A topological model of composite preons." arXiv:hep-ph/0503213.

[8] Smolin, L. (1992). "Did the universe evolve?" *Class. Quant. Grav.* 9(1), 173-191.

[9] 't Hooft, G. (1993). "Dimensional reduction in quantum gravity." arXiv:gr-qc/9310026.

[10] Susskind, L. (1995). "The World as a Hologram." *J. Math. Phys.* 36, 6377.

[11] Penrose, R. (1965). "Gravitational collapse and space-time singularities." *Phys. Rev. Lett.* 14(3), 57-59.

[12] Zurek, W. H. (2003). "Decoherence, einselection, and the quantum origins of the classical." *Rev. Mod. Phys.* 75, 715–775.

[13] Kauffman, L. H. (1991). *Knots and Physics*. World Scientific.

[14] Maxwell, J. C. (1864). "On the calculation of the equilibrium and stiffness of frames." *Phil. Mag.* 27, 294.

[15] Regge, T. (1961). "General relativity without coordinates." *Nuovo Cim.* 19, 558.

[16] Meyer, D. A. (1989). *The Dimension of Causal Sets*. Ph.D. Thesis, MIT.

[17] Sorkin, R. D. (2003). "Causal Sets: Discrete Gravity." arXiv:gr-qc/0309009.

[18] Durhuus, B., Jonsson, T., & Wheater, J. F. (2006). "The spectral dimension of generic trees." *Nucl. Phys. B* 733, 48-63.

[19] Neal, R. M. (1993). "Probabilistic Inference Using Markov Chain Monte Carlo Methods." Technical Report CRG-TR-93-1, University of Toronto.